34th Annual International Conference of the IEEE EMBS
San Diego, California USA, 28 August - 1 September, 2012

Measurement of Retinal Arteriolar Diameters from Auto Scale Phase Congruency with Fuzzy Weighting and L1 Regularization

Joubin Nasehi Tehrani, *Student Member, IEEE*, Hong Yan, *Fellow, IEEE,* Meidong Zhu, Craig Jin, Alistair L McEwan, *Senior Members, IEEE*

***Abstract*— Manual measurements of small changes in retinal vascular diameter are slow and may be subject to considerable observer-related biases. Among the conventional automatic methods the sliding linear regression filter (SLRF) demonstrates the least scattered and most repeatable coefficients. For optimal performance it relies on the choice of the correct filter scale for different vessel sizes. A small scale extracts fine details at the expense noise sensitivity, while large scales have poor edge localization. Here we use auto scale phase congruency to select the filter scales with fuzzy weighting to reduce noise, and L1 regularization for edge smoothing. Our method uses a one dimensional analysis normal to the vessel and so is faster than the 2D phase congruency. In 65 vessels randomly selected from 20 images the proposed method showed better repeatability and over three times less scattering than conventional SLRF.**

I. Introduction

IT has been shown that changes in retinal vessel diameter are an important sign for diseases such as hypertension, arteriosclerosis and diabetes [1-3]. Manual quantification of retinal vascular changes is difficult for several reasons: the low image contrast between vessels and background, presence of noise, variation of vessel radius, brightness, curvature, and shape. In addition, manual methods are slow and subject to observer bias. For quantification of vascular changes several automatic methods have been proposed. Full width half-maximum (FWHM) or half-height at full-width (HHFW) was introduced by Brinchmann-Hansen, which measures the width of retinal vessels recorded using microdensitometric methods [4, 5]. Zhou et al. experimented with Gaussian fitting functions to estimate vessel width and they reported promising results using a Gaussian model [6]. Gregson *et al*. introduced an alternative approach, comprising of a rectangular profile of a fixed height that is fitted to the profile data [7]. Chapman *et al.* compared three methods of automated vascular measurements (Gaussian function, Sobel edge detection and SLRF) with manually recorded vessel diameters [8]. They reported that the Gaussian function performed poorly in comparison with SLRF method. Marr and Hildreth in 1980 [9] have argued that the Gaussian is an optimal filter for edge detection because of its localization properties in both the spatial and the frequency domains. Since then, the Gaussian has been widely used in retinal image studies. Gang and his group evaluated the fitness of estimating vessel profiles with the Gaussian function and proposed an amplitude-modified second-order Gaussian filter for the detection and measurement of vessels [10]. Zhang and his group proposed a matched filter (MF) approach, namely the MF-FDOG (first-order derivative of Gaussian), to detect retinal blood vessels. This method was composed of a zero-mean Gaussian function, and its first-order [11]. Zhu [12] presented a method to detect vessels based on symmetry in the Fourier domain. They measured symmetry using the scale-invariant property and the phase congruency model. This method is effective in the presence of thin and thick vessels and invariant to brightness variations of the vessel. However, it is ineffective in the presence of a wide range of vessels, and requires optimal parameter values or a combination of predefined models.

Figure 1. Retinal photograph. The white line on image shows the manually selected cut of a normal vessel near the macula.

Figure 1 shows a fundus photograph of an eye with a typical selection of a normal vessel near the macula. Typical slice has been demonstrated in Figure 2 where I_0 is the grey level intensity at the vessel relative to the average retinal background and I_r is the intensity of the light reflex. The width of the blood column, w_0 and the width of the light streak, w_r are measured at the level of half minimum, $(1/2I_0)$ and at half maximum $(1/2I_r)$ intensities [13].

Supported by an Australian government Postgraduate Award (APA). Analysis of retinal images with approval of South Eastern Sydney and Illawarra Area Health Service – Northern Network Human Research Ethics Committee, HREC ref no: 05/175.

J. Nasehi Tehrani, C. Jin, and A. McEwan, are with the School of Electrical and Information Engineering, The University of Sydney, Australia, NSW 2006; (phone: +612 9351 7581; e-mail: joubin.nasehitehrani@sydney.edu.au).

M. Zhu is with the Save Sight Institute, Sydney Eye Hospital Campus, University of Sydney; (e-mail: meidong.zhu@sydney.edu.au).

H. Yan is with the Department of Electronic Engineering, City University of Hong Kong; (e-mail: h.yan@cityu.edu.hk).

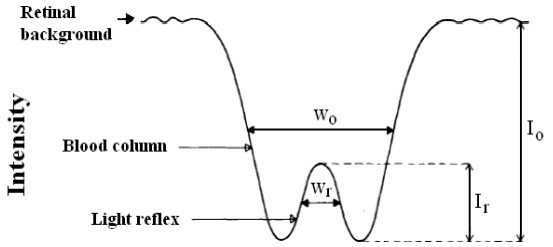

Figure 2. A schematic pixel intensity of scan parameters in a densitometric profile across a retinal vessel [13]. $\boldsymbol{W_0}$ is the width of the blood column.

One of the difficulties in measuring the vessel diameter using edge detectors is that any linear filtering on a densitometric profile across a retinal vessel suppresses noise and also blurs the significant transitions. The amount of smoothing applied depends on the size or scale of the smoothing operator. Large scales extract coarse details with a large localization error. Besides, finding a single scale of smoothing which is optimal for all vessel diameters in a single retinal image is very difficult. In order to solve this problem, Jeong and Kim [14] proposed a scheme which automatically determines the optimal scales for each pixel before detecting the final edge map by defining an energy function that quantitatively determines the usefulness of the possible edge map. However, this method showed a poor result for detecting straight lines in vertical or horizontal directions and very low speed performance. Deng and Cahill [15] use an adaptive Gaussian filtering for edge detection. In this method variance of the Gaussian filter adapts to the noise characteristics and the local variance of the image data. The disadvantage of this method is that it assumes the noise is Gaussian with known variance. In this research, we used a new method based on L1 regularization to find the optimum filter scales which trade-off the noise with the edge localization error (smoothing error) of the signal. The edge detections are based on phase congruency with the Gabor function [16-17]. We also change the weighting factor of the phase congruency algorithm to a fuzzy weighting to attenuate its response to noise in an area away from the region of interest. Our comparison of the new algorithm with the SLRF method shows an improvement in the standard deviation of measured vessel diameter.

II. OUR APPROACH

A. Edge extraction based on phase congruency

Phase congruency is a multi-scale dimensionless quantity used to extract signal and image features that are invariant to change in brightness or contrast. Kovesi [16] defines phase congruency by the following equation:

$$PC(x) = \frac{\sum_o (W_o(x)(E_o(x) - T_o)^+)}{\varepsilon + \sum_o \sum_n A_{no}(x)} \qquad (1)$$

where, $(\,)^+$ denotes that the difference between the functions is not permitted to become negative, x is the one dimensional signal, o is the index of orientation, $W_o(x)$ is the weighting factor, ε is a small value to avoid division by zero (for the result of this paper the value is 0.001), T_o is a threshold for estimating noise, $\sum_n A_{no}(x)$ is the sum of the wavelet response amplitudes in each orientation, and $E_o(x)$ is the local energy function. The frequency ranges (the wavelet scales) over which phase congruency is determined are selected by a regularization algorithm which will be explained in section C. We allowed seven wavelet scales (the selected scale and three scales larger and three scales smaller than the selected one) with a ratio of 1.2 between successive filters. If we let M_n^e and M_n^o denote the even and odd wavelets at scale n, $\sum_n A_n(x)$ the sum of the amplitudes of the frequency components is given by

$$\sum_n A_n(x) = \sum_n \sqrt{(I(x) * M_n^e)^2 + (I(x) * M_n^o)^2} \qquad (2)$$

$I(x)$ denotes the pixel intensity of densitometric profile across a retinal vessel (Figure 2).

The local energy also is defined for a one dimensional profile as

$$E_o = \sqrt{(\sum_n I(x) * M_n^e)^2 + (\sum_n I(x) * M_n^o)^2}. \qquad (3)$$

In our study the orientation of the signal is defined by a line perpendicular to the selected vessel. This line is drawn manually and its alignment is updated to maximize orthogonality using the Matlab commands "getline", and "improfile" that return pixel-value cross-sections along line segments. Figure 3 illustrates the result of a typical one dimensional signal after applying an even filter, an odd filter, and our fuzzy weighted phase congruency.

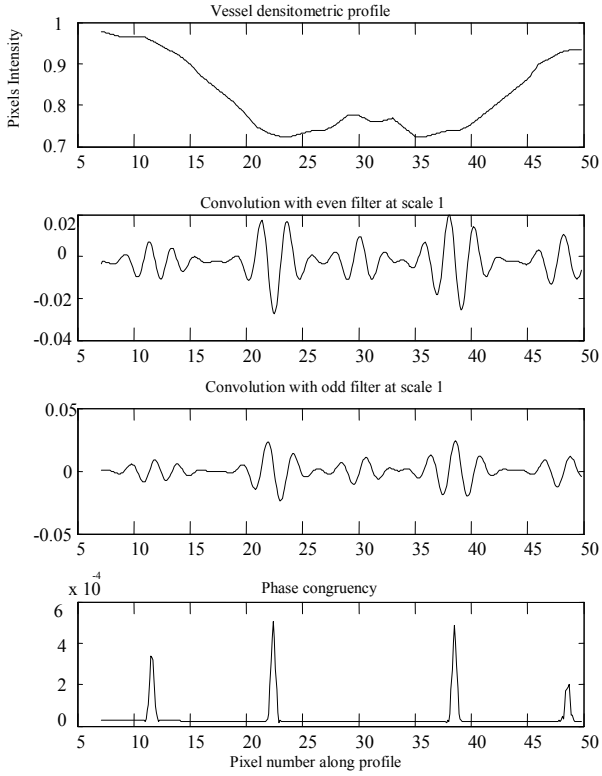

Figure 3. Comparison of algorithms applied to typical retinal vessel profile (top). The second graph is the output of the even filter, the third one is the output of odd filter and the fourth one is our phase congruency result.

B. Weighting

A difficulty with phase congruency is its response to noise [16]. In Equation (1) the effect of noise is bounded by subtraction of a threshold from the local energy. However, the pixel intensity inside the densitometric profile as shown in Figure 3 is not as sharp as the step profiles. For solving

this problem we use a weighting factor which combining the weighting by frequency spread [16] and two sigmoid curve membership functions (Figure 4). For every selected vessel we used the frequency spread weighting function. For pixel intensities less than the average the coefficients were multiplied by the descending sigmoid membership function and for larger than average, they were multiplied by the ascending sigmoid curve. The typical graph of phase congruency coefficients when weighted by these fuzzy rules is demonstrated in figure 3.

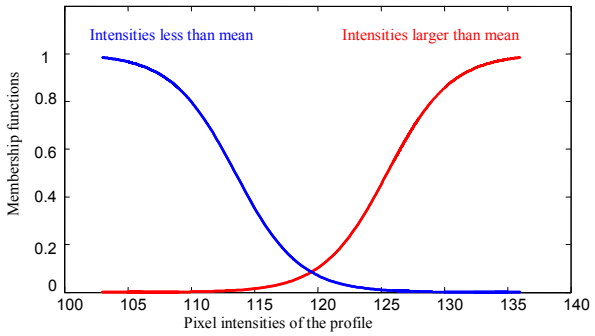

Figure 4. Sigmoid membership functions used to weight the phase congruency coefficients. The average pixel intensity in this graph is 117.

C. *L1 trend estimating*

In noise filtering, the variance of the observed signal (vessel densitometric profile) is related to original signal with the following relation:

$$\sigma_I^2(x) = \sigma_f^2(x) + \sigma_n^2(x) \quad (4)$$

where I is the observed signal, f is the original signal and n is the noise. In order to adapt the variance of filter scale (σ) to the local variance of signal, a possible solution is to use the local variance of the original signal denoted as σ_f^2, which also needs to be estimated or assumed. In this paper we propose a regularization algorithm [18- 20] to determine the optimum filter scale. This method is based on an optimization problem with two competing objectives. We can choose the trend estimate y as the minimize of the objective function

$$min \frac{1}{2}\|G_\sigma * I - y\|_2^2 + \lambda\|Dy\|_1 \quad (5)$$

where $\|u\|_1 = \sum_i |u_i|$ denotes the L1 norm of the vector u, $\|u\|_2 = (\sum_i u_i{}^2)^{1/2}$ is the Euclidean or L2 norm, D is the second-order difference matrix, G_σ is the Gaussian filter with scale of σ which convolve with the observed signal, and $\lambda \geq 0$ is the regularization parameter used to control the trade-off between smoothness of trend and the size of residual $(G_\sigma * I - y)$. The L1 trend filtering method produces trend estimates that are piecewise linear, and therefore is well suited to analyzing time series with an underlying piecewise linear trend. Figure 5 demonstrates L1 trend estimation of a typical densitometric profile across a retinal vessel by regularization parameter $\lambda = 0.05$ and $\sigma = 0$. The value of λ is related to the result of estimated trend. As λ decreases to zero the level of smoothing is zero and the estimated trend becomes smoother by increasing λ.

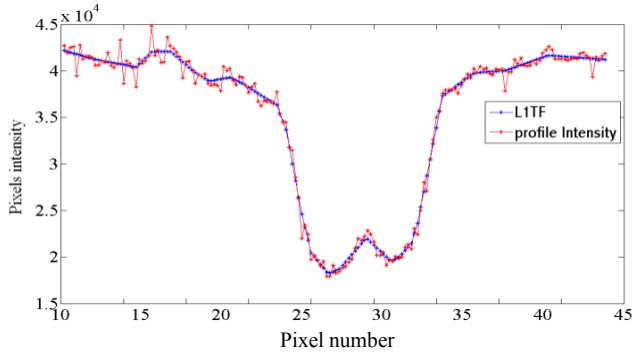

Figure 5. The red graph shows a typical noisy densitometric profile and the blue graph is the L1 trend estimation with $\lambda = 0.05$ and $\sigma = 0$.

Figure 6 shows the typical changes of mean square error related to the smoothing level of selected vessel profile by increasing filter scale. As the filter scale σ increases, the fitting error which related to smoothness level of the filtered signal decreases.

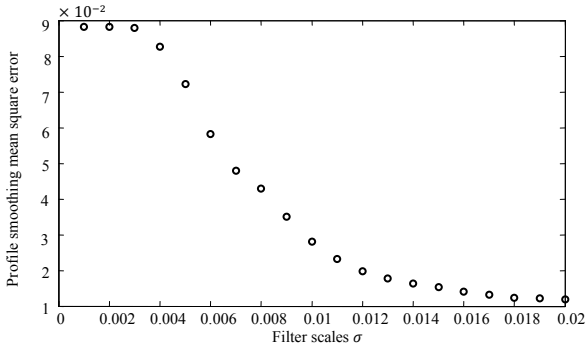

Figure 6. Estimated error curve with the L1 trend algorithm for different filter scales.

III. METHODS

Twenty color fundus retinal images were obtained from normal and healthy people in the study from the Save Sight Institute (Sydney Eye Hospital Campus, University of Sydney). The images were captured by TOPCON (TRC-50IX) and the digitized image dimensions were 4896×3252 pixels (the width of each pixel is $2.5\mu m$). From this database 65 vessels were selected randomly. The line normal to each vessel was selected manually. The median diameter in ten parallel cross sections of the selected slice was measured with one pixel spacing between each cross section. Ten times up-sampling and interpolation of the profile was performed to include changes smaller than a fraction of a pixel [21]. The vessel diameter calculated with two automatic methods: 1) the proposed algorithm and 2) the conventional SLRF. These were compared to manual calculation of HHFW. The mean difference in the diameter calculated by the automatic methods and the manual calculation of HHFW were evaluated with 95% limits of agreement $(2 \times SD)$ and shown graphically as Bland-Altman plots [22].

IV. STATISTICAL ANALYSIS

Figure 7 and 8 demonstrated Bland-Altman plots for the SLRF and proposed algorithm. The mean differences (95% limits of agreement) between the diameters measured manually and SLRF was 2.81 pixels and for the proposed method was 0.77 pixels. The repeatability coefficients for each technique $2.77 \times S_w$ (S_w standard deviation for median diameter determination for each method [8]) were 9.56 for SLRF and 4.22 for proposed method.

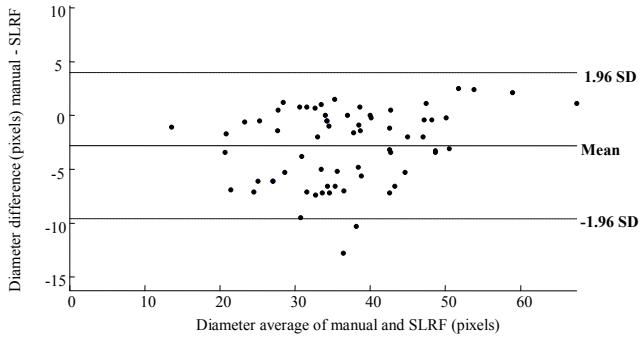

Figure 7. Bland-Altman plots of difference between median manual and median SLRF diameter measurements.

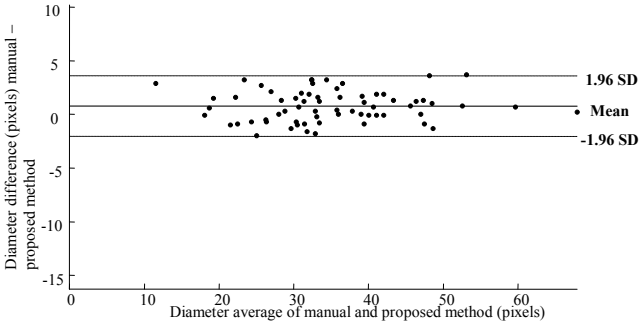

Figure 8. Bland-Altman plots of the difference between median manual and median proposed method of diameter measurements.

V. CONCLUSION

In this paper, we have described an effective approach for boundary detection of retinal vessel using cross-sectional profiles. The proposed algorithm uses auto scale Gabor filters to extract the edge information based on phase congruency. Using one dimensional signal analysis on a selected orientation (normal to the vessels) increases the speed of calculation, as the computational burden is less than 2D phase congruency which tries to find the maximum modulus of the transform as pixel features over several orientations. In our approach, we used retinal vessels from normal and healthy people. Hence we assume that the profile trend is piecewise linear and fit the optimum filter scale by adjusting the regularization parameter. The next step in our study will be evaluating the method on unhealthy patients as their vessels may have some vascular abnormalities such as exudation, or abnormal vessel walls that could impact on our piecewise linear estimation. Our method is effective for a wide range of vessels diameters and can be used to calibrate the retinal vascular changes in diabetic retinopathy, macular telangiectasia, and age-related macular degeneration. This method could be useful for retinal image sequences analysis [23] with little operator intervention.

ACKNOWLEDGEMENTS

Professor Mark Gillies (Sydney Eye Hospital) for subject data and Andrea Padoan (University Hospital of Padua, Italy) the author of Bland-Altman plot Matlab code.

REFERENCES

[1] T. Y. Wong, "Hypertensive retinopathy," *N. Engl. J. Med.*, vol.351,pp. 2310–2317, 2004.

[2] R. Klein, "The relation of systemic hypertension to changes in the retinal vasculature: The Beaver Dam eye study," *Trans. Amer. Ophthalmological Soc*., vol.95, pp. 329-350, 1997.

[3] D. C. Klonoff, D. M. Schwartz, "An economic analysis of interventions for diabetes," *Diabetes Care*, vol.23, no.3, pp. 390–404, 2000.

[4] O. Brinchmann-Hansen, "Theoretical relationships between light streak characteristics and optical properties of retinal vessels," *Acta Ophthalmol Suppl.* vol. 179, pp. 33-37, 1986.

[5] O. Brinchmann-Hansen, "Microphotometry of the blood column and light streak on retinal vessels in fundus photographs," *Acta Ophthalmologica, Suppl.*, vol.179, pp. 9-19, 1986.

[6] L. Zhou, "The detection and quantification of retinopathy using digital angiograms," *IEEE Trans. Med. Imag.*, vol.13, no.4, pp. 619-626, 1994.

[7] P. H. Gregson, "Automated grading of venous beading. *Comput. Biomed. Res.*, vol. 28, pp. 291-304, 2000.

[8] N. Chapman, "Computer algorithms for the automated measurements of retinal arteriolar diameters," *Br. J. Ophthalmol.*, vol.85, pp. 75-79, 2001.

[9] D. Marr, and E. Hildreth, "Theory of edge detection," Proc. R. Soc. Lond. A, *Math Phys. Sci.*, 1980. B 207, pp. 187-217.

[10] L. Gang, "Detection and Measurement of Retinal Vessels in Fundus Images Using Amplitude Modified Second Order Gaussian Filter," *IEEE trans. Biomed. Eng.*, vol. 49, no.2, pp. 168-172, 2002.

[11] B. Zhang, "Retinal vessel extraction by matched filter with first-order derivative of Gaussian," *Elsevier Computers in Biology and Medicine*, vol.40, pp. 438-445, 2010.

[12] T. Zhu, " Fourier cross-sectional profile for vessel detection on retinal images," *Comp. Med. Imag. and Graph.* vol. 34, pp. 203-212, 2010.

[13] O. Brinchmann-Hansen, "Fundus photography of width and intensity profiles of the blood column and the light reflex in retinal vessels," *Acta Ophthalmol. Suppl.* vol. 179: pp. 20-28, 1986.

[14] H. Jeong and C. I. Kim, "Adaptive determination of filter scales for edge detection," *IEEE Trans. Pattern Anal. Machine Intel*., vol. 14, PP. 579-585, May 1992.

[15] G. Deng and L. W. Cahill, "An adaptive Gaussian filter for noise reduction and edge detection," *in Proc. IEEE Nucl. Sci. Symp. Med. Im. Conf.*, PP.1615-1619, 1994.

[16] P. Kovesi., "Image features from phase congruency," *Journal of Computer Vision Research*, vol. 1, no. 3,pp. 1–26, 1999.

[17] J. Nasehi Tehrani, C. Wang, C. Jin, A. L. McEwan,"Edge enhancement for retinal vasculature caliber evaluation in prediction of cardiovascular disease", *Int. Conf. BMEI*, Shanghai, pp.210-213, 2011.

[18] S. J. Kim, "L1 trend filtering," *Siam Review*, problems and techniques section, vol.51, no.2: pp. 339-360, 2009.

[19] J. Nasehi Tehrani, A. McEwan, C. Jin, A. van Schaik, "L1 regularization method in electrical impedance tomography by using the L1-curve (Pareto frontier curve)," *Appl. Math. Modelling*, vol. 36, no. 3, pp.1095–1105, 2012.

[20] J. Nasehi Tehrani, C. Jin, A. McEwan, A. van Schaik,"A comparison between compressed sensing algorithms in electrical impedance tomography", *Conf Proc IEEE Eng Med Biol Soc.*, pp.3109-3112, 2010.

[21] M. Ashraful Amin, Hong Yan,"High speed detection of retinal blood vessels in fundus image using phase congruency". *Soft Comput.* vol.15, no.6, pp.1217-1230, 2011.

[22] J. M. Bland, "Measuring agreement in method comparison studies," *Statistical Methods in Medical Research*, vol. 8, no. 2, pp. 135-160, 1999.

[23] M. J. Dumskyj, "The accurate assessment of changes in retinal vessel diameter using multiple frame electrocardiograph synchronized fundus photography," *Current Eye Research*, pp.625-632. 1996.